This article was downloaded by: [Renmin University of China]
On: 13 October 2013, At: 10:27
Publisher: Taylor & Francis
Informa Ltd Registered in England and Wales Registered Number: 1072954 Registered office: Mortimer House, 37-41 Mortimer Street, London W1T 3JH, UK

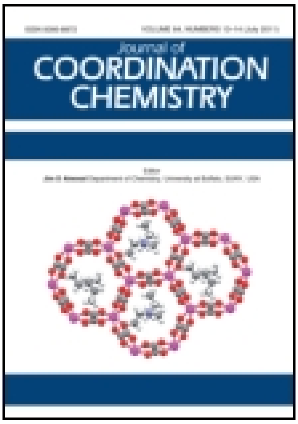

Journal of Coordination Chemistry
Publication details, including instructions for authors and subscription information:
http://www.tandfonline.com/loi/gcoo20

Three 1-D molybdenum(V) phosphates with copper/nickel coordination cations

Xiao-Hua Chen [a] [b] , Shen Lin [a] [b] , Jiao-Hua Liu [a] , Hua Huang [a] , Ming-Xing Yang [a] [b] & Li-Juan Chen [a] [b]

[a] College of Chemistry and Materials, Fujian Normal University , Fuzhou 350007, China

[b] State Key Laboratory of Structural Chemistry, Fujian Institute of Research on the Structure of Matter, Chinese Academy of Sciences , Fuzhou, Fujian 350002, China

Published online: 03 Oct 2011.

To cite this article: Xiao-Hua Chen , Shen Lin , Jiao-Hua Liu , Hua Huang , Ming-Xing Yang & Li-Juan Chen (2011) Three 1-D molybdenum(V) phosphates with copper/nickel coordination cations, Journal of Coordination Chemistry, 64:20, 3482-3494, DOI: 10.1080/00958972.2011.622376

To link to this article: http://dx.doi.org/10.1080/00958972.2011.622376

PLEASE SCROLL DOWN FOR ARTICLE

Taylor & Francis makes every effort to ensure the accuracy of all the information (the "Content") contained in the publications on our platform. However, Taylor & Francis, our agents, and our licensors make no representations or warranties whatsoever as to the accuracy, completeness, or suitability for any purpose of the Content. Any opinions and views expressed in this publication are the opinions and views of the authors, and are not the views of or endorsed by Taylor & Francis. The accuracy of the Content should not be relied upon and should be independently verified with primary sources of information. Taylor and Francis shall not be liable for any losses, actions, claims, proceedings, demands, costs, expenses, damages, and other liabilities whatsoever or howsoever caused arising directly or indirectly in connection with, in relation to or arising out of the use of the Content.

This article may be used for research, teaching, and private study purposes. Any substantial or systematic reproduction, redistribution, reselling, loan, sub-licensing, systematic supply, or distribution in any form to anyone is expressly forbidden. Terms &

Journal of Coordination Chemistry
Vol. 64, No. 20, 20 October 2011, 3482–3494

Taylor & Francis
Taylor & Francis Group

Three 1-D molybdenum(V) phosphates with copper/nickel coordination cations

XIAO-HUA CHEN†‡, SHEN LIN*†‡, JIAO-HUA LIU†,
HUA HUANG†, MING-XING YANG†‡ and LI-JUAN CHEN†‡

†College of Chemistry and Materials, Fujian Normal University, Fuzhou 350007, China
‡State Key Laboratory of Structural Chemistry, Fujian Institute of Research on the Structure of Matter, Chinese Academy of Sciences, Fuzhou, Fujian 350002, China

(*Received 1 May 2011; in final form 26 August 2011*)

Three 1-D reduced molybdenum(V) phosphates, $[Ni(OH)_2][Na_2(H_2O)_3]_2\{Ni[(MoO_2)_6(OH)_3(HPO_4)_3(PO_4)]_2\}\cdot 2C_6H_{14}N_2\cdot 2H_3O\cdot 5H_2O$ (**1**), $[Ni(H_2O)_2][K(H_2O)_5]_2\{Ni[(MoO_2)_6(OH)_3(HPO_4)_3(PO_4)]_2\}\cdot 2C_6H_{14}N_2\cdot 2H_3O\cdot 4H_2O$ (**2**), and $[Cu(H_2O)_2][Na(H_2O)_5]_2\{Cu[(MoO_2)_6(OH)_3(HPO_4)_3(PO_4)]_2\}\cdot 2C_6H_{14}N_2\cdot 2H_3O\cdot 4H_2O$ (**3**), have been hydrothermally synthesized and structurally characterized by single-crystal X-ray diffraction. The crystallographic analysis reveals that **1** is based on $\{Ni[Mo_6O_{12}(OH)_3(HPO_4)_3(PO_4)]_2\}$ clusters connected through $\{[Ni(OH)_2][Na_2(H_2O)_3]_2\}$ pentanuclear mixed-metal cluster units to yield unusual 1-D chains along the *c*-axis, which further form 3-D supramolecular networks *via* hydrogen-bonding. Compounds **2** and **3** are heterogeneous isostructural compounds. Both are built from $M[Mo_6P_4]_2$ (M = Ni or Cu) blocks as the structural motif combined with $[MO_4(H_2O)_2]$ (M = Ni or Cu) octahedra to form 1-D chains, where $M[Mo_6P_4]_2$ (M = Ni or Cu) is bonded by $[M'(H_2O)_5]$ (M′ = K or Na). Furthermore, bulk carbon paste electrode modified with **1** (**1-CPE**) displays good electrocatalytic activity toward reduction of nitrite or bromate.

Keywords: Reduced molybdenum(V) phosphates; Hydrothermal synthesis; Electrocatalytic activity

1. Introduction

Inorganic–organic materials with 1-D, 2-D, and 3-D frameworks have attracted much attention due to structural flexibility and applications in molecular absorption, catalysis, photochemistry, and electromagnetism [1–7]. A challenge in this field is the designed synthesis of new structural types based on polyoxometalates. Metal oxide clusters based on anionic molybdenum phosphates as a new class of solid materials have attracted attention for their abundant structures and uses in catalysis and materials science, especially for reduced molybdenum phosphates. Some reduced molybdenum phosphates have been reported [8, 9], in which hydrothermal synthesis, in combination with templates have been demonstrated to be an effective strategy. Most of these compounds with 1-D, 2-D, and 3-D microporous or tunnel structures possess basic building units $M[Mo_6P_4]_2$($[Mo_6P_4] \equiv [P_4Mo_6O_{28-x}(OH)_{3+x}]^{(9-x)-}$), such as $Na[Mo_6P_4]_2$

---

*Corresponding author. Email: shenlin@fjnu.edu.cn

Journal of Coordination Chemistry
ISSN 0095-8972 print/ISSN 1029-0389 online
http://dx.doi.org/10.1080/00958972.2011.622376

unit [10–13], Zn[Mo_6P_4]$_2$ unit [14–17], Co[Mo_6P_4]$_2$ unit [18–22], Fe[Mo_6P_4]$_2$ unit [23–27], and Cd[Mo_6P_4]$_2$ unit [28–32]. Only a few molybdenum(V) phosphates containing nickel have been reported [33–36]. In the compounds above, M[Mo_6P_4]$_2$ fragments are linked by dinuclear [13], trinuclear [18], or tetranuclear metal clusters [20].

In this article, we report the hydrothermal synthesis and crystal structures of three 1-D molybdenum(V) phosphates $[Ni(OH)_2][Na_2(H_2O)_3]_2\{Ni[(MoO_2)_6(OH)_3(HPO_4)_3(PO_4)]_2\} \cdot 2C_6H_{14}N_2 \cdot 2H_3O \cdot 5H_2O$ (**1**), $[Ni(H_2O)_2][K(H_2O)_5]_2\{Ni[(MoO_2)_6(OH)_3(HPO_4)_3(PO_4)]_2\} \cdot 2C_6H_{14}N_2 \cdot 2H_3O \cdot 4H_2O$ (**2**), and $[Cu(H_2O)_2][Na(H_2O)_5]_2\{Cu[(MoO_2)_6(OH)_3(HPO_4)_3(PO_4)]_2\} \cdot 2C_6H_{14}N_2 \cdot 2H_3O \cdot 4H_2O$ (**3**). These compounds contain the basic M[Mo_6P_4]$_2$ (M = Ni or Cu) building blocks, in which 1,4-diazabicyclo[2,2,2]octane as organic templating agents has been introduced into the systems. Molybdate phosphates in the presence of 1,4-diazabicyclo[2,2,2]octane as charge-compensating cations have never been reported.

In **2** or **3**, M[Mo_6P_4]$_2$ (M = Ni or Cu) clusters are connected by $M(H_2O)_2$ (M = Ni or Cu) fragments through covalent bonds, resulting in a 1-D chain. In **1**, the basic Ni[Mo_6P_4]$_2$ building blocks are covalently connected by $[Ni(OH)_2][Na_2(H_2O)_3]_2$ pentanuclear metal clusters to yield unusual 1-D chains, which are further linked to form a 3-D supramolecular structure *via* hydrogen-bonding interactions. This is the first example of [Mo_6P_4]$_2$ fragments connecting by centrosymmetric pentanuclear mixed-metal clusters in molybdenum phosphates.

2. Experimental

2.1. *Materials and instrumentation*

All chemicals purchased were of reagent grade and used without purification. Elemental analyses for C, H, and N were carried out with an Elementar Vario EL III microanalyser. IR spectra were recorded on a Perkin-Elmer spectrum 2000 spectrophotometer with KBr pellets from 4000 to 400 cm^{-1}. Cyclic voltammograms were obtained on a CHI-660 electrochemical instrument with a Pt wire auxiliary and Ag/AgCl reference electrode at room temperature. A chemically bulk-modified CPE was used as a working electrode.

2.2. *Synthesis of compounds 1, 2, and 3*

Hydrothermal synthesis of **1**: A mixture of MoO_3 (0.25 mmol), $Ni(CH_3COO)_2 \cdot 4H_2O$ (0.25 mmol), 1,4-diazabicyclo[2,2,2]octane (0.5 mmol), H_3PO_4 (0.5 mL) and H_2O (9 mL) was neutralized to pH $\approx$ 5.0 with 1 mol L^{-1} NaOH under continuous stirring and sealed in a 20 mL Teflon-lined autoclave, then heated to 160°C for 4 days. After cooling to room temperature at 10°C h^{-1}, black crystals were obtained in 15.3% yield based on Mo. Elemental analysis: Calcd for $C_{12}H_{70}Mo_{12}N_4Na_4Ni_2O_{77}P_8$ (%): C, 4.63; H, 2.28; N, 1.81. Found (%): C, 4.59; H, 2.14; N, 1.75. Main IR frequencies (KBr pellets, cm^{-1}): 3429m, ν(O–H); 1627m, ν(N–H); 1150m, υ(P–O); 962s, ν(Mo=O); and 714m, ν(Mo–O–Mo).

Hydrothermal synthesis of **2**: A mixture of MoO_3 (0.25 mmol), $Ni(CH_3COO)_2 \cdot 4H_2O$ (0.25 mmol), 1,4-diazabicyclo[2,2,2]octane (0.5 mmol), H_3PO_4 (0.5 mL) and H_2O (9 mL) was neutralized to pH ≈ 5.0 with 1 molL^{-1} KOH under continuous stirring and sealed in a 20 mL Teflon-lined autoclave, then heated to 160°C for 4 days. After cooling to room temperature at 10°C h^{-1}, black crystals were obtained in 15.3% yield based on Mo. Elemental analysis: Calcd for $C_{12}H_{78}K_2Mo_{12}N_4Ni_2O_{80}P_8$ (%): C, 4.57; H, 2.48; N, 1.77. Found (%): C, 4.46; H, 2.34; N, 1.62. Main IR frequencies (KBr pellets, cm^{-1}): 3415m, ν(O–H); 1615m, ν(N–H); 1148m, υ(P–O); 958s, ν(Mo=O); and 735m, ν(Mo–O–Mo).

Hydrothermal synthesis of **3**: A mixture of MoO_3 (0.25 mmol), $CuCl_2 \cdot 2H_2O$ (0.25 mmol), 1,4-diazabicyclo[2,2,2]octane (0.5 mmol), H_3PO_4 (0.5 mL) and H_2O (9 mL) was neutralized to pH ≈ 5.0 with 1 molL^{-1} NaOH under continuous stirring and sealed in a 20 mL Teflon-lined autoclave, then heated to 160°C for 4 days. After cooling to room temperature at 10°C h^{-1}, black crystals were obtained in 15.3% yield based on Mo. Elemental analysis: Calcd for $C_{12}H_{78}Na_2Mo_{12}N_4Cu_2O_{80}P_8$ (%): C, 4.60; H, 2.51; N, 1.79. Found (%): C, 4.42; H, 2.38; N, 1.65. Main IR frequencies (KBr pellets, cm^{-1}): 3432m, ν(O–H); 1608m, ν(N–H); 1162m, υ(P–O); 975s, ν(Mo = O); and 723m, ν(Mo–O–Mo).

2.3. *Crystal structure determination*

Crystals of **1**–**3** with suitable size were selected for the structure analyses. Intensity data were collected at Bruker SMART-CCD and Rigaku R-AXIS RAPID IP diffractometer with Mo-Kα monochromated radiation (λ = 0.71073 Å) at 293 K. The structures were solved by direct methods with SHELXS-97 [37] and refined by full-matrix least squares calculations with SHELXL-97 [37]. All non-hydrogen atoms were refined anisotropically, except for two disordered oxygen atoms of water in **2** and **3** which were refined isotropically. Positions of the hydrogen atoms attached to carbon in **1**, **2**, and **3**, and hydrogen atoms attached to oxygen atoms O2W and O3W in **1** were fixed in ideal positions, while other hydrogen atoms were not located. A summary of crystallographic data for **1**, **2**, and **3** are given in table 1.

2.4. *Preparation of 1-CPE*

Compound **1** was employed as a modifier to fabricate carbon paste electrode (**1-CPE**). Graphite powder of 200 mg and *ca* 20 mg **1** were mixed and ground together by an agate mortar and pestle to achieve an even, dry mixture. To that mixture, 1 mL paraffin oil was added and stirred with a glass rod. Then the homogeneous mixture was used to pack kryptols, and the surface was wiped with weighing paper.

3. Results and discussion

3.1. *Description of the structures*

3.1.1. Crystal structure of 1. Single-crystal X-ray diffraction analysis reveals that **1** consists of $\{Ni[Mo_6O_{12}(OH)_3(HPO_4)_3(PO_4)]_2\}$ (simplified as $Ni[Mo_6P_4]_2$), $\{[Ni(OH)_2][Na_2(H_2O)_3]_2\}$ pentanuclear mixed-metal cluster unit (simplified as $NiNa_4$), protonated 1,4-diazabicyclo[2,2,2]octane and lattice water molecules. Selected bond lengths and angles are given in table 2.

Table 1. Crystallographic data for **1**–**3**.

	1	**2**	**3**
Empirical formula	$C_{12}H_{70}Mo_{12}N_4Na_4Ni_2O_{77}P_8$	$C_{12}H_{78}K_2Mo_{12}N_4Ni_2O_{80}P_8$	$C_{12}H_{78}Na_2Mo_{12}N_4Cu_2O_{80}P_8$
Formula weight	3111.14	3153.44	3130.8
Crystal size	0.45 × 0.26 × 0.15	0.29 × 0.23 × 0.18	0.33 × 0.15 × 0.09
Crystal system	Triclinic	Triclinic	Triclinic
Space group	$P\bar{1}$	$P\bar{1}$	$P\bar{1}$
Unit cell dimensions (Å, °)			
a	12.287(10)	12.292(2)	12.293(2)
b	13.121(10)	12.973(1)	12.979(2)
c	14.109(10)	14.070(2)	14.077(2)
α	113.602(7)	106.455	106.509(2)
β	100.070(8)	109.130(3)	109.223(2)
γ	108.897(7)	108.461(2)	108.342(2)
Volume (Å^3), Z	1846(2), 1	1813.4(4), 1	1814.7(4), 1
Calculated density (g cm^{-3})	2.798	2.888	2.865
Temperature (K)	293(2)	293(2)	293(2)
Absorption coefficient (mm^{-1})	2.797	2.944	2.906
$F(000)$	1510	1536	1522
θ range for data collection (°)	2.76–28.37	2.55–27.49	2.55–27.48
Index range	$-16 \leq h \leq 16$; $-17 \leq k \leq 17$; $-18 \leq l \leq 18$	$-15 \leq h \leq 15$; $-16 \leq k \leq 16$; $-18 \leq l \leq 16$	$-15 \leq l \leq 15$; $-16 \leq k \leq 16$; $-18 \leq l \leq 18$
Independent reflections	8851 [$R_{int} = 0.0140$]	7742 [$R_{int} = 0.0236$]	7748 [$R_{int} = 0.0245$]
Observed reflections	8286	7146	6950
Number of variables	556	539	540
Final R_1, wR_2 [$I > 2\sigma(I)$]	0.0269, 0.0735	0.0498, 0.1354	0.0596, 0.1848
Final R_1, wR_2 (all data)	0.0292, 0.0748	0.0533, 0.1394	0.0651, 0.1928
Goodness-of-fit on F^2	1.058	1.029	1.169
(Δ/σ)max, mean	0.001, 0.000	0.002, 0.000	0.000, 0.000
$\Delta\rho_{max}/\Delta\rho_{min}$ (e Å^{-3})	2.842 and −1.934	3.830 and −1.838	3.027 and −1.460

As shown in figure 1, [Mo_6P_4] of **1** is made up of six MoO_6 octahedra and four PO_4 tetrahedra, in accord with reduced molybdenum phosphate derivatives reported [38–40]. Each MoO_6 unit contains a Mo=O group and shares two edges with neighboring MoO_6 octahedra. The central phosphate provides three oxygen atoms that bridge the bonding Mo···Mo contacts (avg. 2.59 Å), while each remaining three PO_4 groups has two oxygen atoms to span the non-bonding Mo···Mo contacts (avg. 3.51 Å). Each Mo^{5+} in **1** has a distorted octahedral coordination geometry with an apical Mo = O bond at ~1.68 Å and five other Mo–O bonds with lengths from ~1.94 to ~2.33 Å. Based on valence sum calculations [41], the values for all the molybdenum and phosphorous atoms are ~5.16–~5.26 and ~4.93–~5.02, respectively, indicating that all Mo and P are in the +5 oxidation state. The P–O bond lengths are 1.495(3)–1.580(3) Å and O–P–O bond angles 105.4(2) to 114.5(2)°. The bond valence values of O(1), O(8), O(11), O(18), O(25), and O(27) are ~1.1–~1.2, indicating that they are all hydroxyl groups. The molybdenum hexamer can be formulated as $[(HPO_4)_3(PO_4)(MoO_2)_6(OH)_3]^{6-}$. Two [$Mo_6P_4$] units are combined by a Ni(1)O_6 octahedron bonded to six oxygen atoms from two hexamer ring units. Therefore, a centrosymmetric sandwich-like [Ni(1)$(Mo_6P_4)_2$] dimer is formed (figure 2). Ni(1)–O bond lengths in the dimer are 2.135(3)–2.186(3) Å and O–Ni(1)–O bond angles are 83.9(1)–180.0(1)°.

As illustrated in figure 3(a), Ni(2) is located at a crystallographic center and coordinated by two pairs of μ_3-O (O(5), O(7), and O(5A), O(7A)) (symmetry code: A, $-x+1$, $-y$, $-z$) from four P–O groups belonging to two neighboring dimers and one

Table 2. Selected bond lengths (Å) and angles (°) for **1**.

Mo(1)–O(21)	1.679(3)	Mo(1)–O(29)	1.936(3)
Mo(1)–O(32)	1.996(3)	Mo(1)–O(23)	2.037(3)
Mo(1)–O(18)	2.082(3)	Mo(1)–O(6)	2.312(3)
Mo(1)–Mo(2)	2.588(2)	Mo(2)–O(3)	1.688(3)
Mo(2)–O(29)	1.946(3)	Mo(2)–O(32)	1.968(3)
Mo(2)–O(22)	2.065(3)	Mo(2)–O(27)	2.126(3)
Mo(2)–O(16)	2.239(3)	Mo(3)–O(12)	1.692(3)
Mo(3)–O(30)	1.973(3)	Mo(3)–O(31)	1.936(3)
Mo(3)–O(25)	2.086(3)	Mo(3)–O(19)	2.053(3)
Mo(3)–Mo(5)	2.585(2)	Mo(3)–O(15)	2.329(3)
Mo(4)–O(24)	1.943(3)	Mo(4)–O(4)	1.675(3)
Mo(4)–O(9)	2.068(3)	Mo(4)–O(26)	1.969(3)
Mo(4)–O(15)	2.279(3)	Mo(4)–O(25)	2.118(3)
Mo(4)–Mo(6)	2.595(2)	Mo(5)–O(31)	1.946(3)
Mo(5)–O(13)	1.680(3)	Mo(5)–O(28)	2.054(3)
Mo(5)–O(30)	1.975(3)	Mo(5)–O(16)	2.297(3)
Mo(5)–O(27)	2.098(3)	Mo(6)–O(24)	1.939(3)
Mo(6)–O(10)	1.669(3)	Mo(6)–O(14)	2.052(3)
Mo(6)–O(26)	1.993(3)	Mo(6)–O(6)	2.261(3)
Mo(6)–O(18)	2.105(3)	P(1)–O(6)	1.550(3)
P(1)–O(5)	1.506(3)	P(1)–O(16)	1.548(3)
P(1)–O(15)	1.559(3)	P(2)–O(8)	1.536(3)
P(2)–O(2)	1.501(3)	P(2)–O(23)	1.542(3)
P(2)–O(14)	1.555(3)	P(3)–O(9)	1.533(3)
P(3)–O(1)	1.575(3)	P(3)–O(19)	1.540(3)
P(3)–O(17)	1.499(3)	P(4)–O(11)	1.580(3)
P(4)–O(7)	1.495(3)	P(4)–O(28)	1.552(3)
P(4)–O(22)	1.538(3)	Ni(1)–O(26)	2.135(3)
Ni(1)–O(32)	2.186(3)	Ni(1)–O(30)	2.162(3)
Ni(2)–O(7)	2.093(3)	Ni(2)–O(5)	2.066(3)
Ni(2)–O(20)	2.117(3)		
Mo(6)–O(6)–Mo(1)	99.56(10)	Mo(4)–O(15)–Mo(3)	98.83(11)
Mo(1)–O(18)–Mo(6)	112.98(12)	Mo(6)–O(24)–Mo(4)	83.91(12)
Mo(3)–O(25)–Mo(4)	112.72(12)	Mo(4)–O(26)–Mo(6)	81.84(11)
Mo(5)–O(27)–Mo(2)	112.26(12)	Mo(1)–O(29)–Mo(2)	83.61(11)
Mo(3)–O(30)–Mo(5)	81.80(11)	Mo(3)–O(31)–Mo(5)	83.50(11)
Mo(2)–O(32)–Mo(1)	81.48(11)	Mo(2)–O(16)–Mo(5)	101.27(11)

pair of μ_2-OH (O(20), O(20A)), forming an octahedral $[Ni(2)O_4(OH)_2]$ configuration. The bond valence value for O(20) is ~0.8. There are two Na sites in distorted pentagonal bipyramidal configurations. Each Na(1) is coordinated by two water molecules (O(33), O(34)), four phosphate oxygen atoms (O(5A), O(7), O(11), O(17A)) and one molybdate oxygen atom (O(24A)). Each Na(2) links one water molecule (O(35)), three phosphate (O(2), O(5), O(23)) and two molybdate oxygen atoms (O(6), O(29)), and one μ_2-OH (O(20)). The bond values of O(33), O(34), and O(35) are ~0.1–~0.2. The Na–O bond lengths in the two polyhedra range from ~2.32 to ~2.99 Å. Ni(2) is connected to four adjacent sodium atoms (Na(1), Na(2) and Na(1A), Na(2A)) (symmetry code: A, $-x+1$, $-y$, $-z$) *via* its six O donors, resulting in a centrosymmetric pentanuclear mixed-metal cluster unit $\{[Ni(OH)_2][Na_2(H_2O)_3]_2\}$ (figure 3b). Valence bond calculations confirm that Na and Ni are in +1 and +2 oxidation states, respectively. Therefore, the sodium and nickel coordination cations bonded with $Ni[Mo_6P_4]_2$ should be formulated as $\{[Ni(OH)_2][Na_2(H_2O)_3]_2\}^{4+}$.

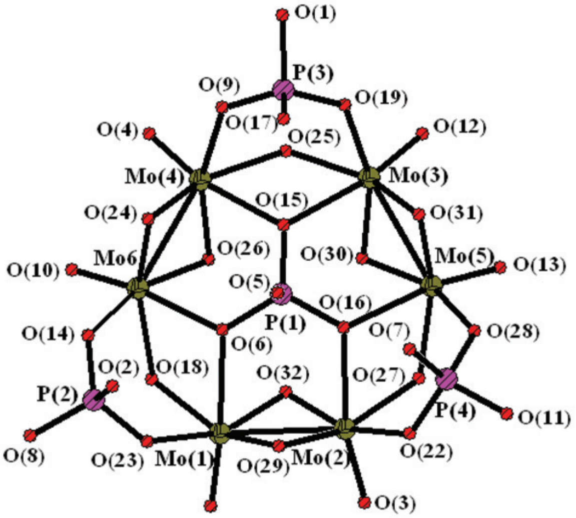

Figure 1. View of [Mo_6P_4] of **1**.

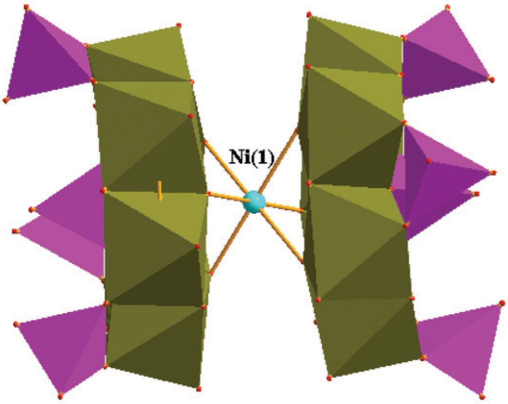

Figure 2. Polyhedral representation of Ni[Mo_6P_4]$_2$ of **1**.

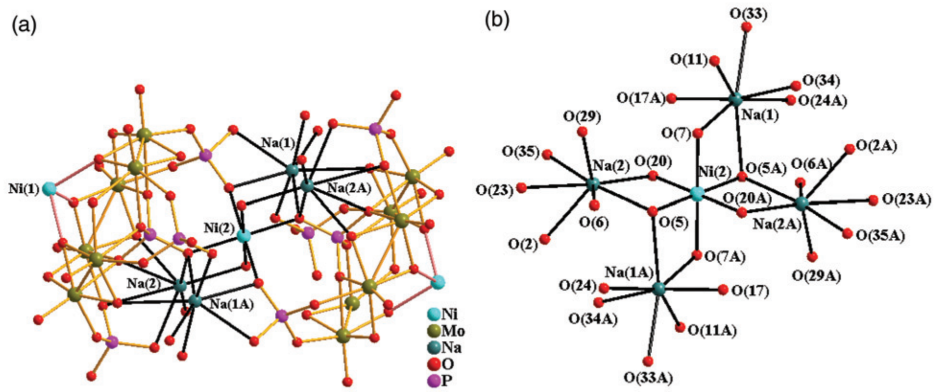

Figure 3. (a) Coordination configurations of four crystallographical independent metals of **1** and (b) view of pentanuclear mixed-metal cluster {[Ni(OH)$_2$][$Na_2(H_2O)_3$]$_2$} of **1** (symmetry code: A, $1-x$, $-y$, $-z$).

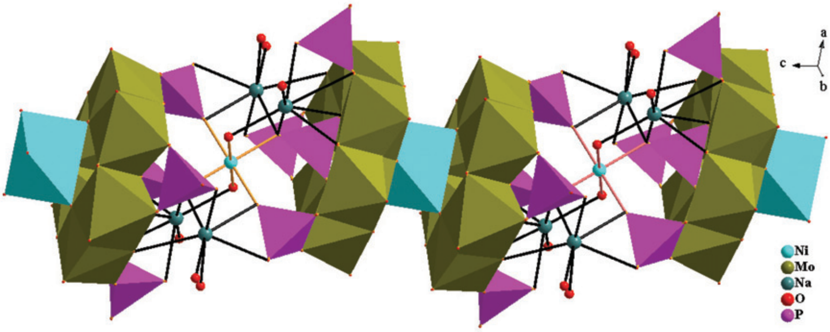

Figure 4. View of the infinite 1-D chain of **1** along the *c*-axis.

Table 3. Hydrogen bonds in **1**.

D–H	*d*(D–H) (Å)	*d*(H···A) (Å)	∠DHA (°)	*d*(D···A) (Å)	A
O2w–H2w1	0.845	2.329	141.44	3.036	O8
O2w–H2w1	0.845	2.562	113.75	3.004	O3[$-x+1$, $-y+1$, $-z+1$]
O2w–H2w2	0.834	2.161	156.55	2.945	O25[x, $y+1$, z]
O3w–H3w1	0.820	1.919	166.28	2.722	O14[$-x$, $-y$, $-z+1$]
O2w–H3w2	0.820	1.983	158.55	2.763	O28[$-x+1$, $-y$, $-z+1$]

As shown in figure 4, Ni(1)$[P_4Mo_6]_2$ units of **1** are connected *via* $\{[Ni(OH)_2][Na_2(H_2O)_3]_2\}$ pentanuclear metal clusters to generate an unusual 1-D chain along the *c*-axis. $M[P_4Mo_6]_2$ fragments linked by dinuclear [13], trinuclear [18] or tetranuclear metal clusters [20] have been reported. However, a connecting mode like **1** has not been reported in molybdenum phosphates. Compound **1** exhibits a 3-D supramolecular framework through extensive hydrogen-bonding interactions among the lattice water molecules and oxygen atoms from molybdenum phosphate anions at distances varying from 2.722 to 3.306 Å (table 3 and figure 5).

3.1.2. Crystal structures of 2 and 3.

X-ray analysis and valence sum calculations show that **2** consists of $\{Ni(1)[Mo_6O_{12}(OH)_3(HPO_4)_3(PO_4)]_2^{6-}\}$ as for **1**, $[Ni(2)O_4(H_2O)_2]$, $[KO(H_2O)_5]$, $[KO(H_2O)_5]$ polyhedra, protonated 1,4-diazabicyclo[2,2,2]octane, and water molecules. Selected bond lengths and angles comparable with those in **1** are given in table 4.

Different from **1**, these $[Ni(1)(Mo_6P_4)_2]$ dimers are linked by one $[Ni(2)O_4(H_2O)_2]$ octahedron to form a 1-D chain (figure 6). The Ni(2) coordinates to two water molecules (O(32), O(32A)) (symmetry code: A, $-x+1$, $-y+1$, $-z+1$), four phosphate oxygen atoms (O(4), O(20) and O(4A), O(20A)) from two $Ni(1)[Mo_6P_4]_2$ clusters, forming an octahedral $[Ni(2)O_4(H_2O)_2]$. K(1) in $[K(H_2O)_5]$ is coordinated by one oxygen atom (O(28)) in P(2)–O from a $[Mo_6P_4]$ unit and five coordinated water molecules, resulting in a $[K(1)O(H_2O)_5]$ octahedron. Thus, every $[K(H_2O)_5]$ fragment connects one $[Mo_6P_4]$ fragment *via* K(1)–O(28)–P(2) bridge. Compound **3** possesses similar structural features to **2**. Selected bond lengths and angles for **3** are given in table 5.

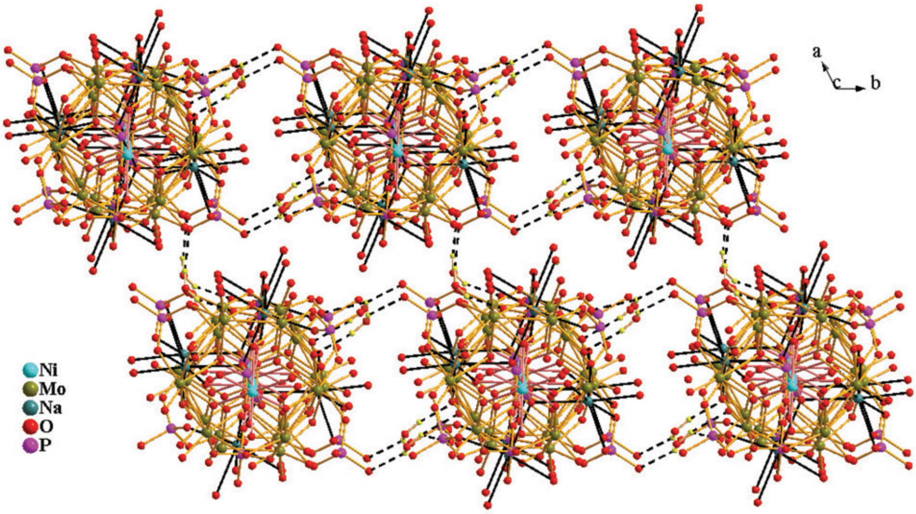

Figure 5. View of the 3-D supramolecular structure of **1** along the *ab* plane.

Table 4. Selected bond lengths (Å) and angles (°) for **2**.

Mo(1)–O(14)	1.672(5)	Mo(1)–O(6)	1.953(5)
Mo(1)–O(5)	1.985(4)	Mo(1)–O(30)	2.056(5)
Mo(1)–O(13)	2.090(5)	Mo(1)–O(3)	2.271(4)
Mo(1)–Mo(2)	2.5890(9)	Mo(2)–O(15)	1.673(5)
Mo(2)–O(6)	1.940(5)	Mo(2)–O(5)	1.981(4)
Mo(2)–O(22)	2.055(5)	Mo(2)–O(7)	2.087(5)
Mo(2)–O(1)	2.265(5)	Mo(3)–O(16)	1.680(5)
Mo(3)–O(8)	1.929(5)	Mo(3)–O(9)	1.973(4)
Mo(3)–O(23)	2.055(5)	Mo(3)–O(7)	2.102(5)
Mo(3)–O(1)	2.285(5)	Mo(3)–Mo(4)	2.5838(8)
Mo(4)–O(17)	1.678(6)	Mo(4)–O(8)	1.945(5)
Mo(4)–O(9)	1.979(4)	Mo(4)–O(26)	2.054(5)
Mo(4)–O(10)	2.099(5)	Mo(4)–O(2)	2.266(4)
Mo(5)–O(18)	1.683(5)	Mo(5)–O(11)	1.929(4)
Mo(5)–O(12)	1.987(4)	Mo(5)–O(27)	2.050(5)
Mo(5)–O(10)	2.089(5)	Mo(5)–O(2)	2.300(5)
Mo(5)–Mo(6)	2.5819(8)	Mo(6)–O(19)	1.689(5)
Mo(6)–O(11)	1.931(4)	Mo(6)–O(12)	1.980(4)
Mo(6)–O(21)	2.075(4)	Mo(6)–O(13)	2.115(4)
Mo(6)–O(3)	2.222(4)	P(1)–O(4)	1.499(5)
P(1)–O(2)	1.550(5)	P(1)–O(3)	1.553(5)
P(1)–O(1)	1.561(5)	P(2)–O(28)	1.507(6)
P(2)–O(29)	1.515(5)	P(2)–O(27)	1.539(6)
P(2)–O(26)	1.545(6)	P(3)–O(21)	1.536(5)
P(3)–O(20)	1.476(5)	P(3)–O(31)	1.574(5)
P(3)–O(30)	1.543(5)	P(4)–O(22)	1.529(7)
P(4)–O(25)	1.522(6)	P(4)–O(23)	1.532(6)
P(4)–O(24)	1.534(6)	Ni(1)–O(9)	2.115(4)
Ni(1)–O(5)	2.114(4)	Ni(2)–O(20)	2.047(5)
Ni(1)–O(12)	2.181(4)	Ni(2)–O(32)	2.091(6)
Ni(2)–O(4)	2.091(5)		
Mo(2)–O(1)–Mo(3)	99.22(17)	Mo(4)–O(2)–Mo(5)	98.91(17)
Mo(6)–O(3)–Mo(1)	101.21(17)	Mo(2)–O(5)–Mo(1)	81.51(16)
Mo(2)–O(6)–Mo(1)	83.37(18)	Mo(2)–O(7)–Mo(3)	111.7(2)
Mo(3)–O(8)–Mo(4)	83.66(19)	Mo(3)–O(9)–Mo(4)	81.66(16)
Mo(5)–O(10)–Mo(4)	111.9(2)	Mo(5)–O(11)–Mo(6)	83.96(17)
Mo(6)–O(12)–Mo(5)	81.22(16)	Mo(1)–O(13)–Mo(6)	111.3(2)

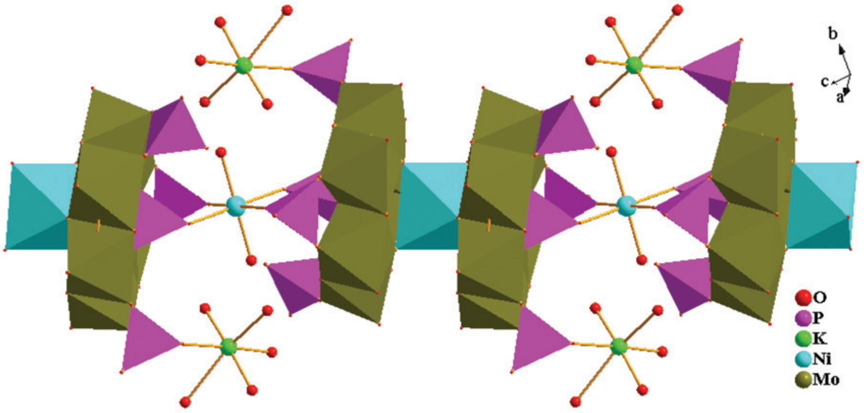

Figure 6. View of the infinite 1-D chain structure of **2**.

Table 5. Selected bond lengths (Å) and angles (°) for **3**.

Mo(1)–O(14)	1.687(6)	Mo(1)–O(5)	1.935(5)
Mo(1)–O(6)	1.987(5)	Mo(1)–O(30)	2.079(6)
Mo(1)–O(13)	2.113(5)	Mo(1)–O(2)	2.231(5)
Mo(1)–Mo(2)	2.5823(9)	Mo(2)–O(15)	1.680(6)
Mo(2)–O(5)	1.931(6)	Mo(2)–O(6)	1.989(5)
Mo(2)–O(22)	2.050(6)	Mo(2)–O(7)	2.087(5)
Mo(2)–O(4)	2.299(5)	Mo(3)–O(16)	1.672(7)
Mo(3)–O(9)	1.941(7)	Mo(3)–O(8)	1.990(5)
Mo(3)–O(23)	2.050(6)	Mo(3)–O(7)	2.116(6)
Mo(3)–O(4)	2.261(5)	Mo(3)–Mo(4)	2.5832(10)
Mo(4)–O(17)	1.691(6)	Mo(4)–O(9)	1.925(6)
Mo(4)–O(8)	1.983(6)	Mo(4)–O(26)	2.051(7)
Mo(4)–O(10)	2.093(6)	Mo(4)–O(1)	2.277(5)
Mo(5)–O(18)	1.680(6)	Mo(5)–O(12)	1.946(6)
Mo(5)–O(11)	1.986(5)	Mo(5)–O(27)	2.056(6)
Mo(5)–O(10)	2.098(6)	Mo(5)–O(1)	2.272(5)
Mo(5)–Mo(6)	2.5900(10)	Mo(6)–O(19)	1.667(6)
Mo(6)–O(12)	1.957(6)	Mo(6)–O(11)	1.985(6)
Mo(6)–O(21)	2.059(6)	Mo(6)–O(13)	2.094(6)
Mo(6)–O(2)	2.279(5)	Cu(1)–O(11)	2.107(6)
Cu(1)–O(8)	2.107(5)	Cu(1)–O(6)	2.180(5)
Cu(2)–O(20)	2.053(6)	Cu(2)–O(3)	2.080(6)
Cu(2)–O(32)	2.096(7)	P(1)–O(3)	1.511(6)
P(1)–O(2)	1.545(5)	P(1)–O(4)	1.551(6)
P(1)–O(1)	1.565(6)	P(2)–O(29)	1.517(7)
P(2)–O(27)	1.539(8)	P(2)–O(26)	1.536(8)
P(2)–O(28)	1.549(8)	P(3)–O(20)	1.484(6)
P(3)–O(21)	1.544(6)	P(3)–O(30)	1.532(6)
P(3)–O(31)	1.574(6)	P(4)–O(25)	1.494(7)
P(4)–O(24)	1.512(7)	P(4)–O(22)	1.539(6)
P(4)–O(23)	1.547(7)		
Mo(5)–O(1)–Mo(4)	99.3(2)	Mo(1)–O(2)–Mo(6)	100.7(2)
Mo(3)–O(4)–Mo(2)	111.5(3)	Mo(2)–O(5)–Mo(1)	83.8(2)
Mo(1)–O(6)–Mo(2)	80.98(19)	Mo(2)–O(7)–Mo(3)	111.5(3)
Mo(4)–O(8)–Mo(3)	81.1(2)	Mo(4)–O(9)–Mo(3)	83.8(2)
Mo(5)–O(10)–Mo(4)	111.7(2)	Mo(5)–O(11)–Mo(6)	81.4(2)
Mo(5)–O(12)–Mo(6)	83.1(2)	Mo(6)–O(13)–Mo(1)	111.3(3)

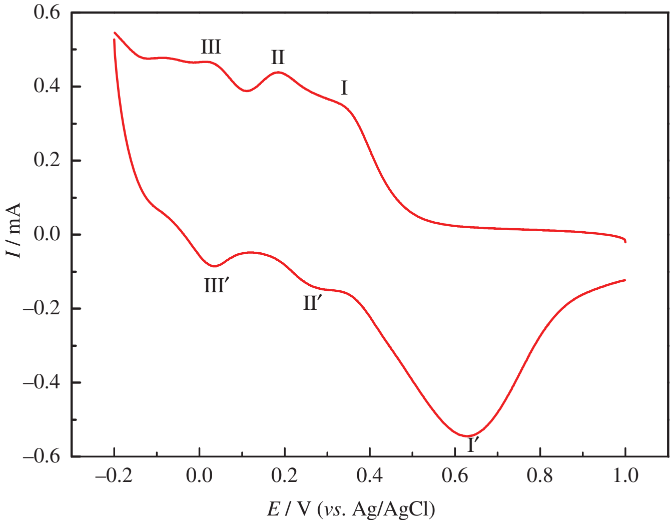

Figure 7. Cyclic voltammograms of the **1-CPE** in 1 mol L^{-1} H_2SO_4 solution at scan rate of 60 mV s^{-1}.

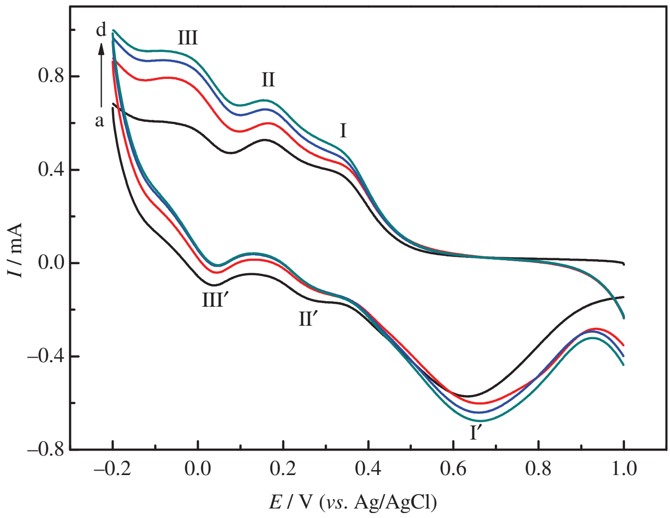

Figure 8. Cyclic voltammograms of **1-CPE** in 1 mol L^{-1} H_2SO_4 solution at 60 mV s^{-1}: (a) the absence of $NaNO_2$; (b) 5.0 mmol L^{-1}$NaNO_2$; (c) 10.0 mmol L^{-1} $NaNO_2$; and (d) 15.0 mmol L^{-1} $NaNO_2$.

3.2. *Electrochemical behavior of 1-CPE*

The cyclic voltammograms for **1-CPE** in 1 mol L^{-1} H_2SO_4 aqueous solution at a scan rate of 60 mv s^{-1} is presented in figure 7. There are three pairs of reversible redox peaks in the potential range +1000 to −200 mV. The half-wave potentials $E_{1/2} = (E_{pc} + E_{pa})/2$ are +485 mV (I), +213 mV (II), and +11 mV (III), respectively (E_{pc} and E_{pa} denote cathodic and anodic peak potentials). The three redox peaks I/I′, II/II′, and III/III′ can be ascribed to two-electron processes of molybdenum.

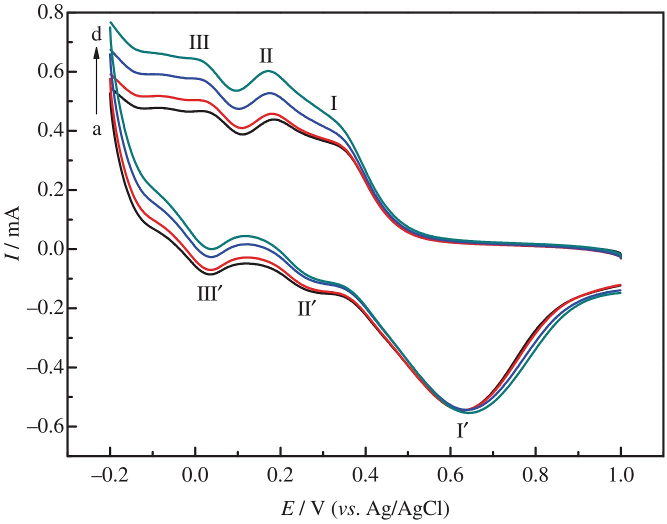

Figure 9. Cyclic voltammograms of **1-CPE** in 1 mol L^{-1} H_2SO_4 solution at 60 mV s^{-1}: (a) the absence of $KBrO_3$; (b) 5.0 mmol $L^{-1}$$KBrO_3$; (c) 10.0 mmol L^{-1} $KBrO_3$; and (d) 15.0 mmol L^{-1} $KBrO_3$.

3.3. *Electrocatalytic activities of the 1-CPE for reduction of NO_2^- and BrO_3^-*

Reduction of nitrite or bromate requires a large overpotential at most electrode surfaces [42]. In our experiment, it was found that **1-CPE** displayed good electrocatalytic activity toward reduction of NO_2^- and BrO_3^- in 1 mol L^{-1} H_2SO_4 solution. As illustrated in figures 8 and 9, the cathodic peak currents increase, while the corresponding anodic peak currents decrease by increasing the concentration of NO_2^- or BrO_3^-. This phenomenon, as expected for a typical electrocatalytic reaction, clearly indicates that reduction of nitrite or bromate is electrocatalyzed by **1-CPE**. Moreover, the increase in cathodic current results from the third molybdenum couple as shown in figure 8, suggesting that it is the third reduced species that catalyzes reduction of NO_2^-; it was the second and the third reduced species that show electrocatalytic activities toward reduction of BrO_3^- simultaneously as shown in figure 9.

4. Conclusion

Three molybdenum(V) phosphates with 1-D chain structure constructed from reduced molybdophosphate $[M(Mo_6P_4)_2]_2$ building blocks have been hydrothermally synthesized. In contrast with other common reduced molybdenum phosphates with $M[Mo_6P_4]_2$ subunits, the molybdenum phosphates in **1–3** are decorated by mixed transition metal moieties. The unusual characteristic of the three complexes is that 1,4-diazabicyclo[2,2,2]octane as an organic templating agent has been introduced into the systems. Compound **1** is the first example of $[Mo_6P_4]_2$ fragments connected by centrosymmetric $\{[Ni(OH)_2][Na_2(H_2O)_3]_2\}$ pentanuclear mixed-metal cluster units in molybdenum phosphates. A 3-D supramolecular network is formed by hydrogen-bonding interaction in **1**. Electrochemical studies indicate that **1** shows potential application in electrocatalysis for reduction of NO_2^- and BrO_3^-.

Supplementary material

Crystallographic data have been deposited with the Cambridge Crystallographic Center with CCDC Nos. 721087, 819948 and 819949. Supplementary data are available from The Director, CCDC, 12 Union Road, Cambridge, CB2 IEZ, UK (Fax: +44-1223-336033; E-mail: deposit@ccdc.cam.ac.uk; www: http://www.ccdc.cam.ac.uk) on request.

Acknowledgments

This work was financially supported by National Science Foundation of China, Grant Nos 20771024 and 21051003, and the Key Project Fund of Science and Technology of Fujian Province, China, Grant No. 2008I0013.

References

[1] O.M. Yaghi, M. O'Keeffe, N.W. Ockwig, H.K. Chae, M. Eddaoudi, J. Kim. *Nature*, **423**, 705 (2003).
[2] L. Han, M.C. Hong, R.H. Wang, J.H. Luo, Z.Z. Lin, D.Q. Yuan. *Chem. Commun.*, 2580 (2003).
[3] N. Calin, S.C. Sevov. *Inorg, Chem.*, **42**, 7304 (2003).
[4] M. Sadakane, E. Steckhan. *Chem. Rev.*, **98**, 219 (1998).
[5] D. Drewes, E.M. Limanski, B. Krebs. *Eur. J. Inorg. Chem.*, 4849 (2004).
[6] M.X. Yang, S. Lin, X.H. Chen, M.H. Luo, J.H. Liu. *J. Coord. Chem.*, **63**, 406 (2010).
[7] M.X. Yang, L.J. Chen, S. Lin, X.H. Chen, H. Huang. *Dalton Trans.*, **40**, 1866 (2011).
[8] X.Q. Chen, S. Lin, L.J. Chen, X.H. Chen, C.L. Liu, J.B. Chen, L.Y. Yang. *Inorg. Chem. Commun.*, **10**, 1285 (2007).
[9] H.X. Guo, S.X. Liu. *J. Mol. Struct.*, **751**, 156 (2005).
[10] M.I. Khan, Q. Chen, J. Zubieta. *Inorg. Chim. Acta*, **206**, 131 (1993).
[11] A. Leclaire, C. Biot, H. Rebbah, M.M. Borel, B. Raveau. *J. Mater. Chem.*, **8**, 439 (1998).
[12] A. Gammersbach, P. Angenault, W.F. Holderich, W. Clegg, M.R.J. Elsegood. *Polyhedron*, **17**, 2535 (1998).
[13] R.D. Huang, F.C. Liu, Y.G. Li, M. Yuan, E.B. Wang, G.H. De, C.W. Hu, N.H. Hu, H.Q. Jia. *Inorg. Chim. Acta*, **349**, 85 (2003).
[14] L.A. Mundi, R.C. Haushalter. *Inorg. Chem.*, **31**, 3050 (1992).
[15] A. Leclaire, A. Guesodon, F. Berrah, M.M. Borel, B. Raveau. *J. Solid State Chem.*, **145**, 291 (1999).
[16] Y. Ma, Y.G. Li, E.B. Wang, Y. Lu, C. Qin, X.X. Xu. *J. Cluster Sci.*, **17**, 167 (2006).
[17] H.X. Guo, J.M. Liu, G.H. Zhu. *J. Coord. Chem.*, **60**, 815 (2007).
[18] H.X. Guo, S.X. Liu. *J. Mol. Struct.*, **741**, 234 (2005).
[19] F.N. Shi, F.A.A. Paz, P.I. Girginova, H.I.S. Nogueira, J. Rocha, V.S. Amaral, A. Makal, J. Klinowski, T. Trindade. *J. Solid State Chem.*, **179**, 1497 (2006).
[20] Y. Ma, Y.G. Li, E.B. Wang, Y. Lu, X.X. Xu. *J. Mol. Struct.*, **791**, 10 (2006).
[21] X. Zhang, J.Q. Xu, J.H. Yu, J. Lu, Y. Xu, Y. Chen, T.G. Wang, X.Y. Yu, Q.F. Yang, Q. Hou. *J. Solid State Chem.*, **180**, 1949 (2007).
[22] Y. Ma, Y.G. Li, E.B. Wang, Y. Lu, X.L. Wang, X.X. Xu. *J. Coord. Chem.*, **60**, 719 (2007).
[23] L.A. Meyer, T.C. Haushalter. *Inorg. Chem.*, **32**, 1579 (1993).
[24] L. Xu, Y. Sun, E.B. Wang, E.H. Shen, Z.R. Liu, C.W. Hu, Y. Xing, Y.H. Lin, H.Q. Jia. *Inorg. Chem. Commun.*, **1**, 382 (1998).
[25] Y.S. Zhou, L.J. Zhang, X.Z. You, S. Natarajan. *J. Solid State Chem.*, **159**, 209 (2001).
[26] H.Z. Shi, Y.K. Shan, M.Y. He, Y.Y. Liu, J.S. Jiang. *J. Mol. Struct.*, **658**, 17 (2003).
[27] L.J. Zhang, Y.S. Zhou, X.Q. Li, Y.H. Li. *J. Cluster Sci.*, **18**, 921 (2007).
[28] A. Leclaire, A. Guesdon, F. Berrah, M.M. Borel, B. Raveau. *J. Solid State Chem.*, **145**, 291 (1999).
[29] A. Leclaire, M.M. Borel, A. Guesdon, R.E. Marsh. *J. Solid State Chem.*, **159**, 7 (2001).
[30] L.Y. Duan, F.C. Liu, X.L. Wang, E.B. Wang, C. Qin, Y.G. Li, X.L. Wang, C.W. Hu. *J. Mol. Struct.*, **705**, 15 (2004).

[31] C.X. Wei, J.X. Chen, Y.B. Huang, T.Y. Lan, Z.S. Li, W.J. Zhang, Z.C. Zhang. *J. Mol. Struct.*, **798**, 117 (2006).
[32] Y. Ma, Y.G. Li, E.B. Wang, Y. Lu, X.L. Wang, D.R. Xiao, X.X. Xu. *Inorg. Chim. Acta*, **360**, 421 (2007).
[33] L. Xu, Y.Q. Sun, E.B. Wang, E.H. Shen, Z.R. Liu, C.W. Hu, Y. Xing, Y.H. Lin, H.Q. Jia. *J. Solid State Chem.*, **146**, 533 (1999).
[34] W.J. Chang, Y.C. Jiang, S.L. Wang, K.H. Lii. *Inorg. Chem.*, **45**, 6586 (2006).
[35] X. Zhang, J.Q. Xu, J.H. Yu, J. Liu, Y. Xu, Y. Chen, T.G. Wang, X.Y. Yu, Q.F. Yang, Q. Hou. *J. Solid State Chem.*, **180**, 1949 (2007).
[36] B.Z. Lin, G.H. Han, B.H. Xu, L. Bai, Y.L. Feng, H. Su. *J. Cluster Sci.*, **19**, 379 (2008).
[37] (a) G.M. Sheldrick. *SHELXS-97*, *Program for X-ray Crystal Structure Solution*, University of Göttingen, Germany (1997); (b) G.M. Sheldrick. *SHELXL-97*, *Program for X-ray Crystal Structure Refinement*, University of Göttingen, Germany (1997).
[38] H.X. Guo, S.X. Liu. *Inorg. Chem. Commun.*, **7**, 1217 (2004).
[39] A. Guesdon, M.M. Borel, A. Leclaire, B. Raveau. *Chem. Eur. J.*, **11**, 1797 (1997).
[40] Y.S. Zhou, L.J. Zhang, X.Z. You, S. Natarajan. *Inorg. Chem. Commun.*, **4**, 699 (2001).
[41] I.D. Brown, D. Altermatt. *Acta Crystallogr. B*, **41**, 244 (1985).
[42] F. Bedioui, S. Trevin, J. Devynck. *J. Electroanal. Chem.*, **377**, 295 (1994).